Supplementary information

Table S1: Correlations between ERO1L expression and clinicopathologic parameters in PDAC patients

Clinicopathological parameter	Total 205	Expression of ERO1L		*P*-value
		Low (n=102, %)	High (n=103, %)	
Age (years)				
< 65	97	51 (52.6)	46 (47.4)	0.486
≥ 65	108	51 (47.2)	57 (52.8)	
Gender				
Male	117	63 (53.8)	54 (46.2)	0.205
Female	88	39 (44.3)	49 (55.7)	
Tumor location				
Head	139	70 (50.4)	69 (49.6)	0.881
Body/tail	66	32 (48.5)	34 (51.5)	
TNM (AJCC)				
Stage I	38	24 (63.2)	14 (36.8)	0.316
Stage II	132	62 (47.0)	70 (53.0)	
Stage III	21	9 (42.9)	12 (57.1)	
Stage IV	14	7 (50.0)	7 (50.0)	
Tumor size				
≤ 3 cm	69	45 (65.2)	24 (34.8)	**0.002**
> 3 cm	136	57 (41.9)	79 (58.1)	
T classification				
T1, 2	42	26 (61.9)	16 (38.1)	0.086
T3, 4	163	76 (46.6)	87 (53.4)	
Lymph node metastasis				
Absent	136	71 (52.2)	65 (47.8)	0.376
Present	69	31 (44.9)	38 (55.1)	
Distant metastasis				
Absent	191	95 (59.7)	96 (50.3)	1.000
Present	14	7 (50.0)	7 (50.0)	
Vascular invasion				
Absent	178	92 (51.7)	86 (48.3)	0.215
Present	27	10 (37.0)	17 (63.0)	
Histological differentiation				
Well	11	9 (81.8)	2 (18.2)	**0.033**
Moderate/poor	194	93 (47.9)	101 (52.1)	

The bold number represents the *P*-values with significant differences. *P* value was calculated by χ^2 test or Fisher's exact test.

Table S2: Univariate analysis of prognostic parameters for survival in PDAC patients

Clinical parameters	HR	95% CI	*P*-value
Expression of ERO1L (high vs. low)	1.606	1.142-2.260	**0.004**
Age (≥ 65 years vs. < 65 years)	1.521	1.077-2.149	**0.017**
Gender (male vs. female)	0.734	0.514-1.047	0.088
Tumor location (head vs. body/tail)	1.019	0.708-1.466	0.920
TNM stage (III-IV vs. I-II)	1.267	1.011-1.588	**0.040**
Tumor size (> 3 cm vs. ≤ 3 cm)	2.141	1.182-3.879	**0.012**
T classification (T3, 4 vs. T1, 2)	1.347	0.869-2.086	0.182
Lymph node metastasis (present vs. absent)	1.487	1.049-2.109	**0.026**
Distant metastasis (present vs. absent)	1.945	1.041-3.634	**0.037**
Vascular invasion (present vs. absent)	1.579	0.969-2.572	0.067
Histological differentiation (moderate/poor vs. well)	2.475	1.011-6.058	**0.047**

HR: Hazard ratio; CI: Confidence interval. The bold number represents the *P* value with significant differences.

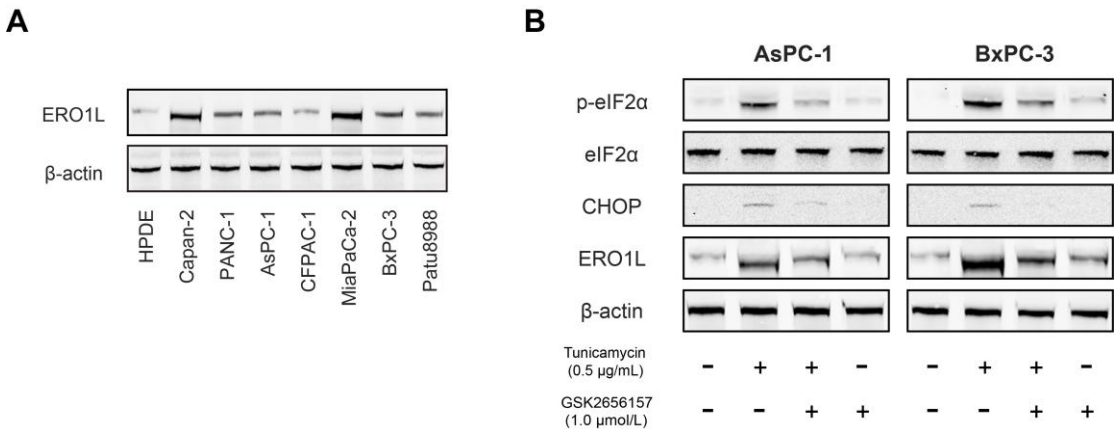

Figure S1. UPR-dependent expression of ERO1L in PDAC cells. (A) Western blotting analysis of ERO1L protein level in seven PDAC cell lines and the non-malignant HPDE cell line; β-actin was used as an internal control. (B) Western blotting analysis of the effect of PERK-EIF2α inhibitor (GSK2656157) on ERO1L protein level in response to Tunicamycin-induced ER stress.

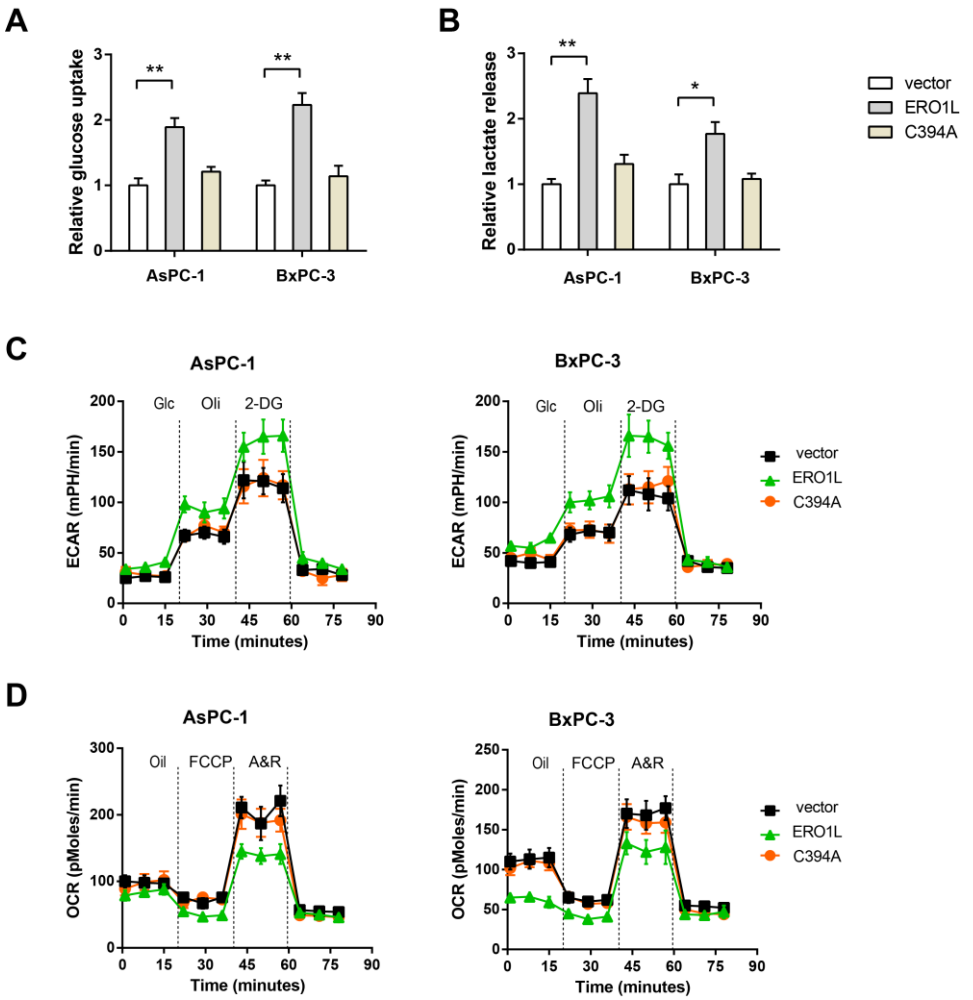

Figure S2. Overexpression of ERO1L promotes the Warburg effect in pancreatic cancer cells. (A) Measurement of glucose uptake in vector, ERO1L-overexpressing and ERO1L-C394A-overexpressing AsPC-1 and BxPC-3 cells (n = 3). (B) Measurement of lactate production in vector, ERO1L-overexpressing and ERO1L-C394A-overexpressing AsPC-1 and BxPC-3 cells (n = 3). (C-D) Detection of the extracellular acidification rate (ECAR, C) and oxygen consumption rate (OCR, D) in vector, ERO1L-overexpressing and ERO1L-C394A-overexpressing AsPC-1 and BxPC-3 cells (n = 3). **P* < 0.05 and ***P* < 0.01.

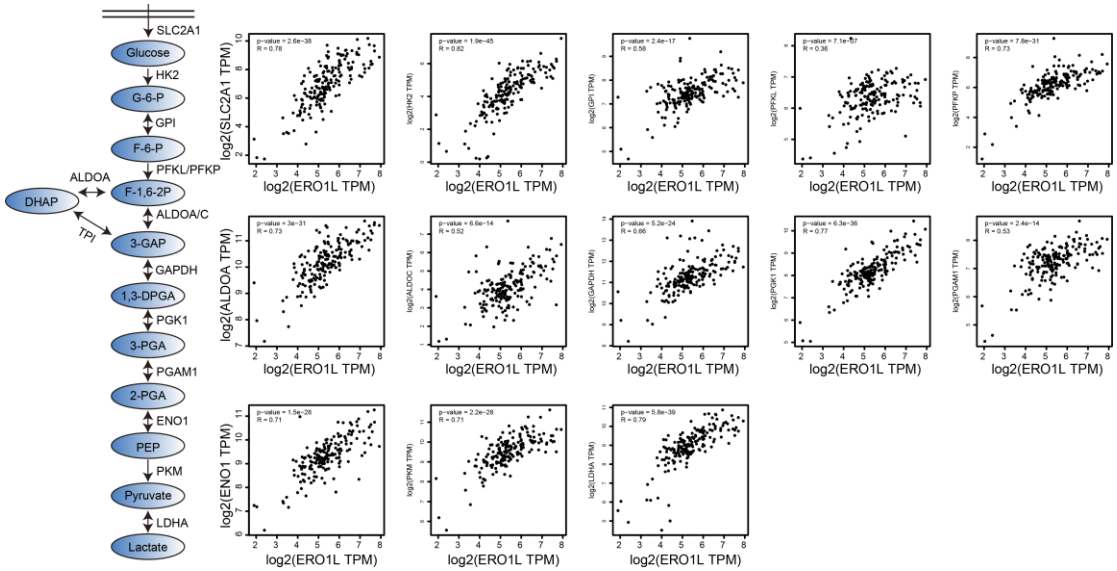

Figure S3. Correlation analysis between ERO1L level and expression of glycolytic components (glucose transporter and glycolytic enzymes) in PDAC samples. Data were derived from TCGA cohort (n = 179).

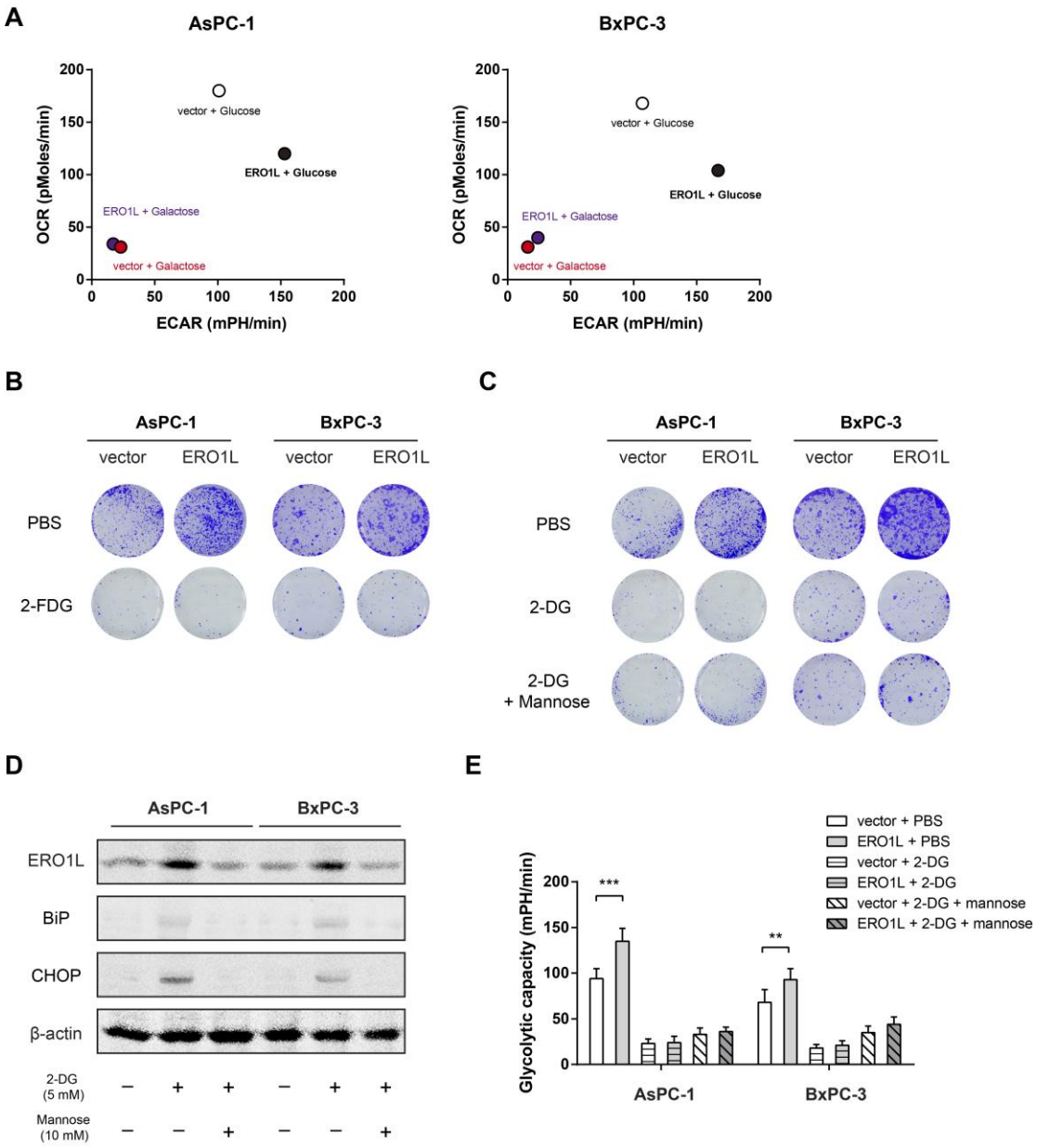

Figure S4. Glycolysis-dependent growth-promoting effect of ERO1L in PDAC. (A) Seahorse analysis of OXPHOS and glycolysis in the presence of galactose by measuring OCR and ECAR in AsPC-1 and BxPC-3 cells (n = 3). (B) Effect of 2-FDG on the plate colony formation ability of ov-vector and ov-ERO1L AsPC1 and BxPC3 cells (n = 3). (C) Effect of 2-DG on the plate colony formation ability of ov-vector and ov-ERO1L AsPC1 and BxPC3 cells in the presence or absence of 10 mM mannose (n = 3). (D) Effect of 2-DG (5 mM) on ER stress and ERO1L expression in the presence or absence of mannose (10 mM). (E) Seahorse analysis of the effect of 2-DG on the glycolytic capacity of AsPC1 and BxPC3 cells in the presence or absence of mannose (n = 9). $^{**}P < 0.01$ and $^{***}P < 0.001$.

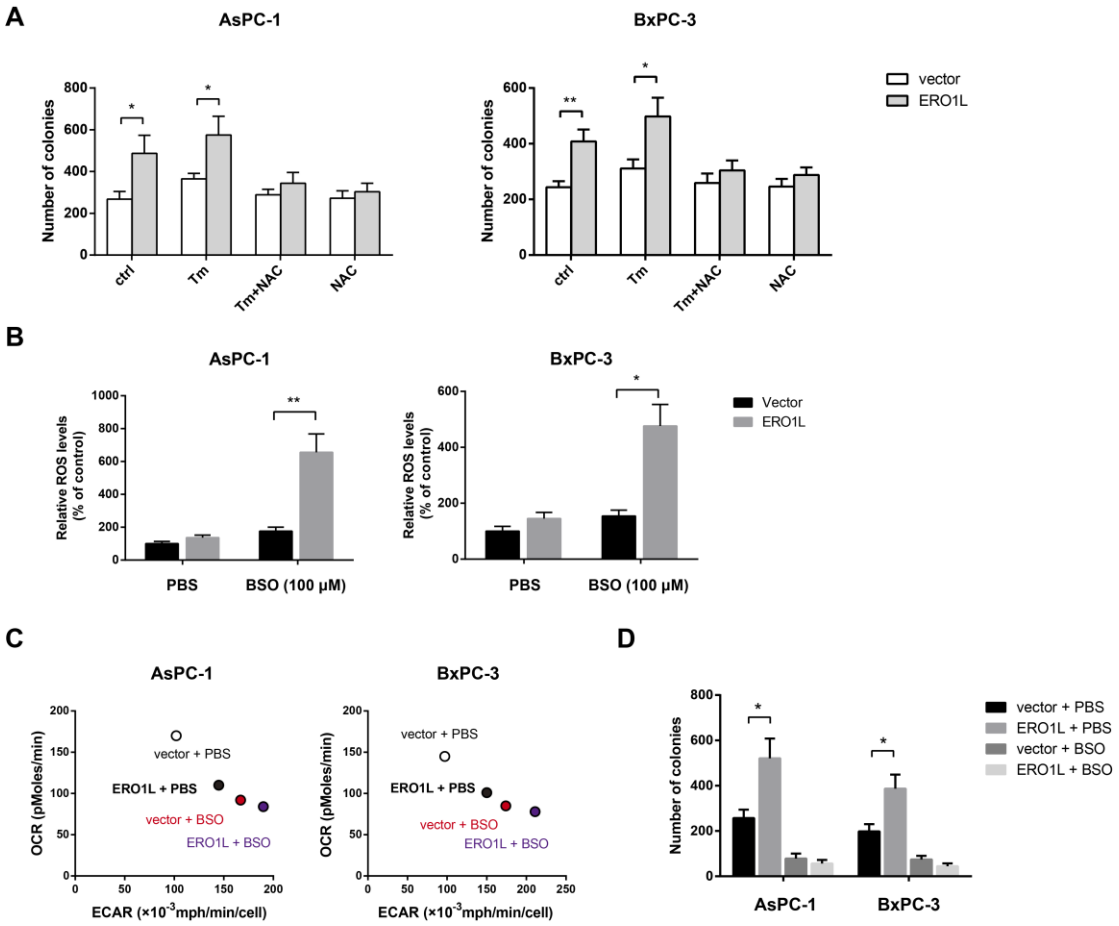

Figure S5. ERO1L oxidoreductase activity is essential for its growth-promoting effect. (A) Neutralizing of ROS levels by N-acetyl cysteine (NAC, 0.2 mM) largely compromised the effect of ERO1L in facilitating tumor growth (n = 3). (B) Effects of GSH inhibitor BSO (100 μM) on ROS generation in ov-vector and ov-ERO1L AsPC-1 and BxPC-3 cells (n = 3). (C) Seahorse analysis of OXPHOS and glycolysis in the presence of BSO treatment (100 μM) by measuring OCR and ECAR in AsPC-1 and BxPC-3 cells (n = 3). (D) Effect of BSO treatment (100 μM) on the plate colony formation ability of ov-vector and ov-ERO1L AsPC-1 and BxPC-3 cells (n = 3). *$P < 0.05$ and **$P < 0.01$.